IC/88/322

INTERNATIONAL CENTRE FOR THEORETICAL PHYSICS

MICROSCOPIC THEORY OF THE PHONON FREQUENCIES IN BCC BARIUM

B.A. Oli

INTERNATIONAL ATOMIC ENERGY AGENCY

UNITED NATIONS EDUCATIONAL, SCIENTIFIC AND CULTURAL ORGANIZATION

IC/88/322

International Atomic Energy Agency
and
United Nations Educational Scientific and Cultural Organization
INTERNATIONAL CENTRE FOR THEORETICAL PHYSICS

MICROSCOPIC THEORY OF THE PHONON FREQUENCIES IN BCC BARIUM *

B.A. Oli **
International Centre for Theoretical Physics, Trieste, Italy.

ABSTRACT

The phonon dispersion frequencies are calculated from first principles for *bbc* barium using a resonance pseudopotential model which incorporates the effect of $s-d$ hybridization. It was also possible using this scheme to account for the anomalous feature of the *Ba* dispersion curve observed experimentally in the $[\xi,0,0]$ direction where the freqencies of the transverse branch are higher than the frequencies of the longitudinal branch. The frequencies obtained were also used to calculate the phonon density of states by the linear–analytic tetrahedra method of zone integration. The results of these calculations are qualitatively in good agreement with experimental data, and provide further support to the interpretation of the anomalous behaviour in the $[\xi,0,0]$ direction as arising from $s-d$ hybridization.

MIRAMARE – TRIESTE
September 1988

* To be submitted for publication.

** Permanent address:Anambra State University of Technology, Awka Campus, P.M.B. 5025, Awka, Anambra State, Nigeria.

1. INTRODUCTION

Recently, Mizuki *et al.* [1] have reported the phonon dispersion curves of *bcc* barium obtained experimentally by the method of inelastic neutron scattering. One of the interesting features of their work which prompted the present calculations, is the surprising result that along the $[\xi,0,0]$ symmetry direction, the frequencies of the longitudinal branch were found to be lower than those of the transverse branch, contrary to the normal behaviour in this symmetry direction. This anomalous feature of the dispersion curve was attributed to the hybridization of the free–electron–like s states with the d bands, which in this metal are just slightly above the Fermi level.

To investigate and possibly provide support for this interpretation, we have embarked on a first principle theoretical calculation of the lattice dynamics of the metal barium using a resonance model potential scheme which incorporates the effect of $s-d$ hybridization. Several calculations [2)–5)] of the dispersion curves of *Ba* have earlier been performed within the framework of the pseudopotential theory of metals. The phonon frequencies calculated by Animalu [2)] and Sharma [3)], using simple local pseudopotentials gave substantially higher frequencies than the experimental values. Furthermore, the calculations were done before the recent experimental results and did not produce the anomalous behaviour in the $[\xi,0,0]$ direction. Morianty [4)] used a generalized pseudopotential approach which attempted to incorporate the effect of $s-d$ hybridization, however, his results also deviated by about 40% as compared to the measured values. Recently Gupta *et al.* [5)] have used an optimised form of model potential to include the influence of hybridization in the phonon frequencies of barium. However, we find their potential in γ–space to be quite unrealistic. In the present calculation, we use a more realistic model potential of the Heine–Abarenkov [6)] type and include the effect of $s-d$ hybridization more consistently in our computation of the electronic bandstructure contribution to the dynamical matrix. In addition, we have calculated also the phonon density of states, which is an important quantity in elucidating the nature of electron–phonon interaction in a given material.

In Section 2, we review the first principles lattice dynamics as applied to a metallic solid. In Section 3, we discuss the model potential used and the modification necessary to include $s-d$ hybridization. In Section 4, the tetrahedral method of calculating phonon density of states is outlined. Finally, in Section 5, the details of the procedure and the results obtained are presented and discussed.

2. OUTLINE OF THE LATTICE DYNAMICS IN METALS

In a microscopic theory of lattice dynamics, within the adiabatic and harmonic approximations, the phonon frequencies (ω) are obtained by solving the dispersion equations:

$$|M\omega^2\delta_{\alpha\beta} - D_{\alpha\beta}(\vec{q})| = 0 \qquad (1)$$

where $\alpha(\text{or}\beta) = 1,2,3$; $\vec{q}$ is the phonon wave–vector and M is the mass of the ion. $D_{\alpha\beta}(\vec{q})$ is the dynamical matrix which is the Fourier transform of the force constants, and for metallic states is made up of three contributions viz:–

$$D_{\alpha\beta}(\vec{q}) = D^C_{\alpha\beta}(\vec{q}) + D^R_{\alpha\beta}(\vec{q}) + D^E_{\alpha\beta}(\vec{q}) \ , \qquad (2)$$

where $D^C_{\alpha\beta}(\vec{q})$ is the contribution due to the direct Coulombic ion–ion interaction;
$D^R_{\alpha\beta}(\vec{q})$ is the repulsive core–core exchange contribution,
and $D^E_{\alpha\beta}(\vec{q})$ is the electronic bandstructure contribution.

The direct Coulombic ion–ion contribution $D^C_{\alpha\beta}$ is calculated in the standard way using the Ewald–Kellerman [7)–8)] method. For the repulsive core–core exchange contribution, we have adopted a Born–Mayer type of potential of the form:

$$V_R(\gamma) = b\ exp[(\gamma_0 - \gamma)/\rho] \qquad (3)$$

where b and ρ are constants given by the volume and compressibility data, and γ_0 is the equilibrium separation between a pair of ions. In this case the elements of the dynamical matrix are as given by Sham [9)]:

$$D^R_{\alpha\beta}(\vec{q}) = \sum_{\ell\neq 0}\left(\frac{b}{\rho}\right) exp[-(\ell-\gamma_0)/\rho]\left\{\left(\frac{1}{\rho}+\frac{1}{\ell}\right)\frac{\ell_\alpha\ell_\beta}{\ell^2} - \frac{\delta_{\alpha\beta}}{\ell}\right\}[1 - exp(i\vec{q}\cdot\vec{\ell})] \ , \qquad (4)$$

where $\{\vec{\ell}\}$ is the set of direct (bcc) lattice vectors.

The electronic bandstructure contribution to the dynamical matrix is calculated here using the expression:

$$D^E_{\alpha\beta}(\vec{q}) = M\omega_\rho^2\left(\sum_{\vec{G}} \frac{(\vec{q}+\vec{G})_\alpha(\vec{q}+\vec{G})_\beta}{|\vec{q}+\vec{G}|^2}\ F(|\vec{q}+\vec{G}|) - \sum_{\vec{G}\neq 0}\frac{\vec{G}_\alpha\vec{G}_\beta}{|\vec{G}|^2}\ F(|\vec{G}|)\right) \qquad (5)$$

where M is the mass of the ion, ω_ρ is the ion plasma frequency, $\vec{G}$ is the reciprocal lattice vector and $F(q)$ is the energy–wave–number characteristic function given in a local approximation by:

$$F(q) = \frac{-\Omega_0 q^2}{8\pi Ze^2}|V_b(q)|^2\frac{\in(q)-1}{|1-f(q)\in(q)} \ . \qquad (6)$$

Here Ω_0 is the atomic volume, Z the valency of the ion, e the electronic charge and $V_b(q)$ is the bare electron–ion potential. $\in(q)$ is the screening dielectric function and $f(q)$ is a correlation and exchange correction function [10)–12)].

3. THE PSEUDOPOTENTIAL AND THE RESONANCE MODEL OF $S-D$ HYBRIDIZATION

It is now generally known that the features of the electronic structure of the divalent alkaline–earth metals Ca, Sr and Ba are intermediate between those of the simple and transition metals. Band theoretical calculations [13)–15)] have established that the d–states are just above the Fermi level and that the electronic wave–functions at E_F contain a substantial admixture of d character arising from $s-d$ hybridization. As a result, the structure and physical properties of a metal like barium is found to be quite sensitive to the d–occupation number.

We therefore incorporate the Ziman [16),17)] resonance model of $s-d$ hybridization in which there is a singular energy dependance of the $\ell=2$ partial wave phase–shift of the form:

$$tan\ \eta_d = \frac{\frac{1}{2}W_d}{E_d - E} \ , \qquad (7)$$

where W_d is the d bandwidth and E_d defines the location of the d band. Thus to handle this singularity in energy at resonance, we have to use a T–matrix type of pseudopotential rather than a V–matrix:

$$T(q) = \frac{2\pi\hbar^3}{\Omega m\sqrt{2mE_F}}\sum_{\ell=0}^{\infty}(2\ell+1)sin\ \eta_\ell\ exp(i\eta_\ell)P_\ell(cos\theta_{kk'}) \ . \qquad (8)$$

In such a model, the d contribution to the T–matrix follows from expression (7) as:

$$exp(i\eta_d)sin\ \eta_d = \frac{-\frac{1}{2}W_d}{(E_d-E)+i\frac{1}{2}W_d} \ , \qquad (9)$$

with a contribution to the form factor $|T(q)|^2$ of the form:

$$sin^2\eta_d = \frac{(\frac{1}{2}W_d)^2}{(E_d-E)^2+(\frac{1}{2}W_d)^2} \ . \qquad (10)$$

In the present calculation, we use the Heine–Abarenkov [16)–20)] type of model potential:

$$V_b(\gamma) = \left.\begin{array}{ll} -\sum_{\ell=0}^{\infty} A_\ell(E)P_\ell & for \quad \gamma \le R_m \\ -\frac{Z_e}{\gamma} & for \quad \gamma > R_m \end{array}\right\} , \qquad (11)$$

where $A_\ell(E)$ are energy dependent well–depths, and $P_\ell = |\ell><\ell|$ are projection operators, and introduce this effect of $s-d$ hybridization through a renormalization of the $\ell=2$ well–depth:–

$$\tilde{A}_2(E) = \frac{\frac{1}{2}\lambda W_d}{(E_d - E + \frac{1}{2}iW_d)} = \lambda sin\ \eta_d\ exp(i\eta_d) \qquad (12)$$

with the constant of proportionality $\lambda = A_d(E_F)(E_d - E_F)$ as in Oli and Animalu [21),22)]. Thus if in a certain energy range such as near the Fermi energy, a resonance corresponding to $s-d$ hybridization occurs, then the $\ell = 2$ (i.e. the d state) contribution to the model potential well-depth has real and imaginary parts given by:

$$Re[\tilde{A}_2(E)] = \frac{(E_d - E)\frac{1}{2}\lambda W_d}{(E_d - E)^2 + (\frac{1}{2}W_d)^2}$$

and

$$I_m[\tilde{A}_2(E)] = \frac{(-\frac{1}{2}W_d)^2\lambda}{(E_d - E)^2 + (\frac{1}{2}W_d)^2}. \qquad (13)$$

It also follows that the renormalized well–depth is given by:

$$\tilde{A}_2 = A_2 cos\ \eta_d\ exp\ i\eta_d = A_2(cos^2\eta_d - i\ sin\ \eta_d\ cos\ \eta_d)$$

and

$$|\tilde{A}_2|^2 = \lambda^2 sin^2\eta_d, \qquad (14)$$

with the value of A_2 being that calculated from the atomic spectroscopic data and extrapolated to E_F, the Fermi energy in the spirit of the quantum defect method.

This resonance effect is illustrated in Fig.1a for the Heine–Abarenkov type of model potential, where the d–states are now delocalized and raised in energy to hybridize with the free conduction s–states. In Fig.1b, we also show the model potential used by Gupta *el al.* [5),23)], to achieve the same effect with two parameters γ_1 and γ_2, their model potential being positive in γ–space inside γ_1, negative from γ_1 to γ_2 and Coulombic outside γ_2. Our model potential is more realistic and directly related to known facts about $s-d$ hybridization with the accompanying resonance type of phase–shift effects in the d–state. For such a scattering by a d–level, an additional density of electronic states is associated with the virtual bound state given by [24)]

$$\delta N_d(E) = \frac{2(2\ell+1)}{\pi}\frac{d\eta_d}{dE} = \frac{10}{\pi}\frac{(\frac{1}{2}W_d)}{(E_d - E)^2 + (\frac{1}{2}W_d)^2}\ , \qquad (15)$$

and this can lead to an appreciable softening in phonon frequencies to produce a lowering of the longitudinal branch in the required direction.

4. PHONON DENSITY OF STATES IN BARIUM

We have also evaluated the phonon density of states $g(\omega)$ for *bcc* barium at 295 K using the linear–analytic tetrahedra method of zone integration [25),26)]. This method originally designed for calculating electronic energy density of states, has been

adapted by us for calculating phonon density of states. This method is better than that of Gilat and Raubenheimer [27)] in the sense that it does not require force constants fit to the dispersion curves, and it does not require the gradients of the frequency curve, rather in the tetrahedron technique, we are only required to know the frequencies at a few reciprocal lattice points of the Brillouin zone. With a suitable interpolation scheme, more values are now generated in the irreducible wedge of the first Brillouin zone, for performing the phonon density of states calculation.

The density of phonon states $g(\omega)$ is defined such that $g(\omega)d\omega$ is the number of phonons per unit cell with frequencies between ω and $\omega + d\omega$ and it is given by the expression:

$$g(\omega) = \frac{\Omega}{(2\pi)^3}\sum_j \int \frac{ds}{|\nabla_q \omega_j(q)|} \qquad (16)$$

where the integral is taken over the surface of constant frequency ω and j is the summation over the different branches. In the linear–analytic tetrahedron method, one divides the irreducible wedge of the Brillouin zone into tetrahedra, and within the i^{th} tetrahedron the frequencies are linearized with respect to some point $\vec{q}_0$ (having a frequency ω_0) at the vertex of the tetrahedron, so that:

$$\omega(\vec{q}) = \omega_0 + \vec{b}\cdot(\vec{q} - \vec{q}_0) \qquad (17)$$

with the coefficient $\vec{b} = [\nabla_q \omega(\vec{q})]_{q_0}$, see Fig.2. In such a case the integral over s in (16) reduces to

$$g(\omega) = \frac{\Omega}{(2\pi)^3}\sum_j \int_s \frac{ds}{|\vec{b}|} = \frac{\Omega}{(2\pi)^3}\frac{1}{|\vec{b}|}\sum_j \int_s ds = \frac{\Omega}{(2\pi)^3}\frac{1}{|\vec{b}|}\sum_{ji} s_{ji}(\omega) \qquad (18)$$

which is just the sum over the tetrahedra, of area of constant frequencies within the tetrahedra.

When the frequencies at the four corners of the i^{th} tetrahedron are ordered such that

$$\omega_0 \le \omega_1 \le \omega_2 \le \omega_3\ ,$$

then the density of frequency states $g_i(\omega)$ from this single tetrahedron is given by the analytic expressions:–

$$g_i(\omega) = \left.\begin{array}{ll} \dfrac{3V_i(\omega-\omega_0)^2}{(\omega_1-\omega_0)(\omega_2-\omega_0)(\omega_3-\omega_0)} & for\quad \omega_0 \le \omega \le \omega_1\ , \\ \dfrac{3V_i}{\Delta}\left[1 - \dfrac{\Delta^2\Delta_m^2}{(\omega_2-\omega_0)(\omega_3-\omega_0)(\omega_2-\omega_1)(\omega_3-\omega_1)}\right] & for\quad \omega_1 \le \omega \le \omega_2\ , \\ \dfrac{3V_i(\omega-\omega_3)^2}{(\omega_3-\omega_0)(\omega_3-\omega_1)(\omega_3-\omega_2)} & for\quad \omega_2 \le \omega \le \omega_3 \end{array}\right\},$$

where V_i = volume of the i^{th} tetrahedron,

$$\Delta = \omega_3 + \omega_2 - \omega_1 - \omega_0,$$
$$\Delta_m = \left[\omega - \frac{(\omega_3\omega_2 - \omega_1\omega_0)}{\Delta}\right].$$

Thus the density of phonon states from one tetrahedron depends only on the frequencies $\omega_0, \omega_1, \omega_2, \omega_3$ at the corners of the tetrahedron and the volume of the tetrahedron and not on the shape of the tetrahedron. A mesh is then constructed in the irreducible wedge of the Brillouin zone, defining the corresponding tetrahedra, before the actual summation is done to give the required density of phonon states.

5. DETAILS OF THE CALCULATIONS, RESULTS AND CONCLUSIONS

Phonon frequencies were computed along the principal symmetry directions for *bcc Ba* by solving the phonon dispersion equation (1). The Born–Mayer parameters for barium used in the calculation are tabulated in Table 1. The only significant contributions to the summation over the lattice vectors in (4) come from the first and second nearest neighbours, and the summation was therefore not extended beyond these. The parameters of the model potential for barium used in Eq.(6) are given in Table 2. The linear screening was done with the Hartree type of dielectric function:

$$E(q) = 1 + \frac{2mZe^2k_F}{\pi\hbar^2q^2}\left[1 + \frac{1-x^2}{2x}\,\ell n\left|\frac{1+x}{1-x}\right|\right], \qquad (18)$$

where $x = q/2k_F$.

The exchange and correlation corrections were included using the modified Hubbard approximation:

$$f(q) = q^2/[2(q^2 + k_F^2 + k_s^2)] \qquad (19)$$

with $k_s^2 = 2k_F/\pi$. The summation over reciprocal lattice vectors in Eq.(5) was performed over 285 reciprocal lattice vectors to ensure proper convergence. The results obtained for the phonon dispersion curves of barium are tabulated in Table 3 and plotted in Fig.3 where they are compared with the experimentally measured phonon frequencies of Mizuki *et al.* [1]. The overall agreement between theory and experiment is good within the framework of a microscopic theory. In particular our model of $s-d$ hybridization produced the same anomalous feature observed experimentally in the $[\xi,0,0]$ direction where the transverse branch are of higher frequencies than the longitudinal branch, between approximately $\xi = 0.2$ to 0.8 wave–vectors. It was also found that if we removed the

resonance effect due to $s-d$ hybridization in our scheme, the normal relative ordering of the branches with longitudinal higher than the transverse branch is restored. We therefore conclude that the first principle calculation of the lattice dynamics of barium presented here is satisfactory enough to justify our support of the view that $s-d$ hybridization between the conduction and unoccupied d band just above the Fermi level is of importance in understanding the occurrence of the relative softening of the longitudinal branch in the $[\xi,0,0]$ dispersion curve of barium.

The phonon density of states $g(\omega)$ for *bcc ba* was also calculated theoretically by the tetrahedral method outlined in Section 4 above, and the result is shown in Fig.4. The overall width and shape of the phonon frequency spectrum and the position of the main peak (at about 2.1 THz) are in good agreement with the results obtained by Mizuki *et al.* [1] using the phenomenological force constant fit method of Gilat and Raubenheimer [27]. However, we have observed that most expermentalists rely on the Born–von Karman force constants model to analyse their data, but a given set of dispersion curves may be fitted with many different sets of such force constants and there is no unique set as such. It is therefore recommended that the tetrahedral method of computing phonon density of states, which only requires the measured phonon frequencies obtained in a few symmetry directions, be used in analysing data obtained experimentally.

ACKNOWLEDGMENTS

The author would like to thank Professor Abdus Salam, the International Atomic Energy Agency and UNESCO for hospitality at the International Centre for Theoretical Physics, Trieste, where most of this work was carried out.

REFERENCES

1) J. Mizuki, Y. Chen, K.M. Ho and C. Stassis, Phys. Rev. **B32**, 666 (1985).

2) A.O.E. Animalu, Phys. Rev. **161**, 445 (1967).

3) K.S. Sharma, Phys. Status Solidi(B), **108**, K101 (1981).

4) J.A. Moriarity, Phys. Rev. **B6**, 4445 (1972).

5) H.C. Gupta, G.S. Reddy, Vijai Baboo Gupta and B.B. Tripathi, Phys. Rev. **B33**, 5839 (1986).

6) V. Heine and I. Abarenkov, Phil. Mag. **9**, 451 (1964).

7) P.P. Ewald, Ann. Phys. Lpz. **64**, 253 (1921).

8) E.W. Kellerman, Phil. Trans. R. Soc. **A238**, 513 (1940).

9) L.J. Sham, Proc. Roy. Soc. **A283**, 33 (1965).

10) J. Hubbard, Proc. Roy. Soc. **A243**, 336 (1958).

11) D.J.W. Geldart and S.H. Vasko, Can. J. Phys. **44**, 2137 (1966).

12) K.S. Singwi, M.P. Tosi, R.H. Land and A. Sjolander, Phys. Rev. **176**, 589 (1968).

13) B. Vasvari, A.O.E. Animalu and V. Heine, Phys. Rev. **B154**, 535 (1967).

14) G. Johansen, Solid State Commun. **7**, 731 (1969).

15) H.L. Skriver, Phys. Rev. Lett. **49**, 1768 (1982).

16) J.M. Ziman, Proc. Phys. Soc. **86**, 337 (1965).

17) V. Heine, Phys. Rev. **153**, 673 (1967).

18) V. Heine and I. Abarenkov, Phil. Mag. **9**, 451 (1964).

19) I. Abarenkov and V. Heine, Phil. Mag. **12**, 529 (1965).

20) A.O.E. Animalu, Phys. Rev. **B8**, 3542 (1973).

21) B.A. Oli and A.O.E. Animalu, Phys. Rev. **B13**, 2398 (1976).

22) A.O.E. Animalu, Phys. Rev. **B10**, 4964 (1974).

23) S. Nand, B.B. Tripathi and H.G. Gupta, Phys. Lett. **53A**, 229 (1975).

24) J.A. Moriarity, Phys. Rev. **B5**, 2066 (1972).

25) O. Jepsen and O.K. Andersen, Solid State Commun. **9**, 1763 (1971).

26) G. Lehmann and M. Taut, Phys. Stat. Solidi(b) **54**, 469 (1972).

27) G. Gilat and L.J. Raubenheimer, Phys. Rev. **144**, 390 (1966).

TABLE CAPTIONS

Table 1 Born–Mayer parameters for barium.

Table 2 Model potential parameters for barium (all quantities in atomic units except where otherwise indicated) (see Ref.13).

Table 3 Measured and calculated phonon frequencies of *bcc Ba* (in THz).

Table 1

b(erg)	$\gamma_0 = 2\gamma_\beta$ γ_β = ionic radius	ρ (cm)	Lattice constant $a(\AA)$
1.50×10^{-12}	2.86×10^{-8}	0.4×10^{-8}	5.01

Table 2

A_0	A_1	A_2	R_m	Ω	Z	m^*	R_c	E_c	ω_p	M	α_{eff}
0.47	0.41	0.99	3.4	424.1	2	1.0	2.70	0.074	2.8×10^{13} (Hz)	2.28×10^{-24} gm	0.097

E_F (Ref.14)	W_d (Ref.14)	E_d (Ref.14)
0.23 (Ryd)	0.05 (Ryd)	0.26 (Ryd)

Table 3

[ξ00]	L		T	
q	Exp.	Theory	Exp.	Theory
0.1	0.28	0.27	0.31	0.30
0.2	0.56	0.40	0.65	0.61
0.3	0.82	0.85	0.98	0.98
0.4	1.05	1.18	1.24	1.28
0.5	1.22	1.25	1.52	1.40
0.6	1.44	1.48	1.73	1.71
0.7	1.74	1.65	1.93	1.80
0.8	2.01	1.80	2.05	1.90
0.9	2.10	1.92	2.15	1.95
1.0	2.15	2.00	2.15	2.00

[ξξ0]	L		T_1		T_2	
q	Exp.	Theory	Exp.	Theory	Exp.	Theory
0.1	0.60	0.50	0.27	0.32	0.47	0.42
0.2	1.25	1.38	0.50	0.45	0.88	0.90
0.3	1.80	1.70	0.65	0.54	1.23	1.25
0.4	2.10	1.80	0.76	0.60	1.44	1.47
0.5	2.30	1.90	0.75	0.78	1.53	1.41

Table 3 (cont.)

[ξξξ]	L		T	
q	Exp.	Theory	Exp.	Theory
0.1	0.78	0.70	–	0.30
0.2	1.56	1.58	0.80	0.71
0.3	2.12	1.98	1.16	0.90
0.4	1.97	1.93	1.47	1.35
0.5	1.72	1.42	1.72	1.50
0.6	1.40	1.20	1.90	1.70
0.7	1.11	1.01	1.99	1.82
0.8	1.36	1.35	2.05	1.90
0.9	1.9)	1.94	2.08	1.92
1.0	–	2.01	–	2.00

FIGURE CAPTIONS

Fig.1a Heine–Abarenkov model potential showing delocalized d–states.

Fig.1b Model potential of Nand, Tripathi and Gupta [23] used by Gupta *et al.* [5].

Fig.2 Geometry for the intersection of the plane of constant $\omega(\vec{q})$ with a tetrahedron defined by the vectors $\vec{q}_0, \vec{q}_1, \vec{q}_2, \vec{q}_3$. The plane shown is that for which $\omega_0 \leq \omega(\vec{q}) \leq \omega_1$, with $\vec{q}_0$ as the origin.

Fig.3 Calculated (continuous curves) and measured (0 •) phonon frequency dispersion curves for *bcc* barium at 295 K.

Fig.4 Phonon density of states $g(\omega)$ of *bcc* barium at 295 K evaluated with the tetrahedron method described in the text.

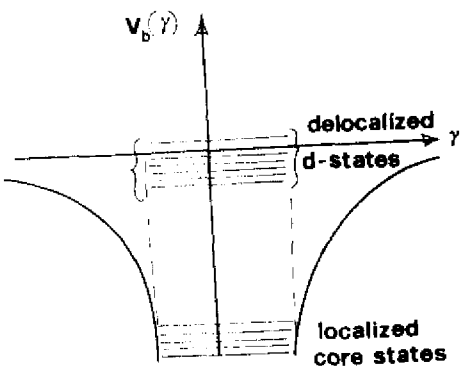

Fig.1a

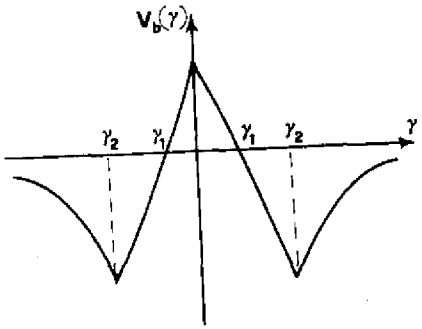

Fig.1b

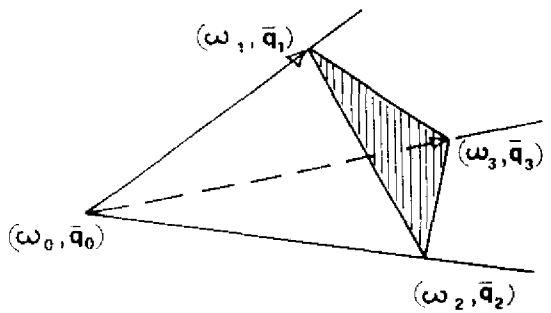

Fig.2

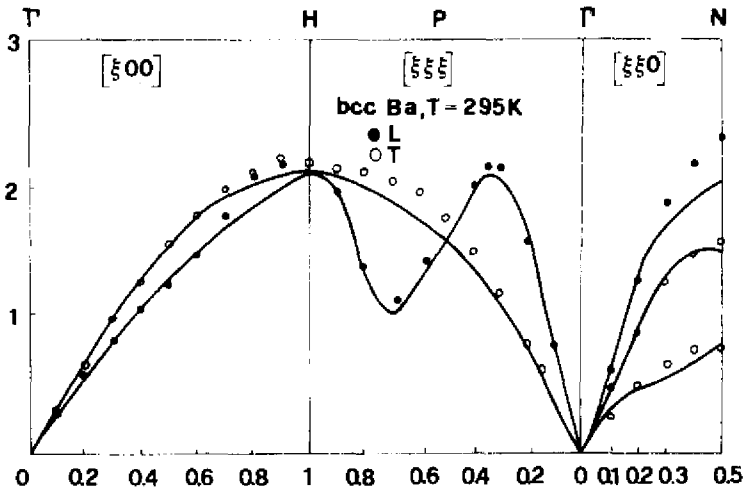

Fig.3

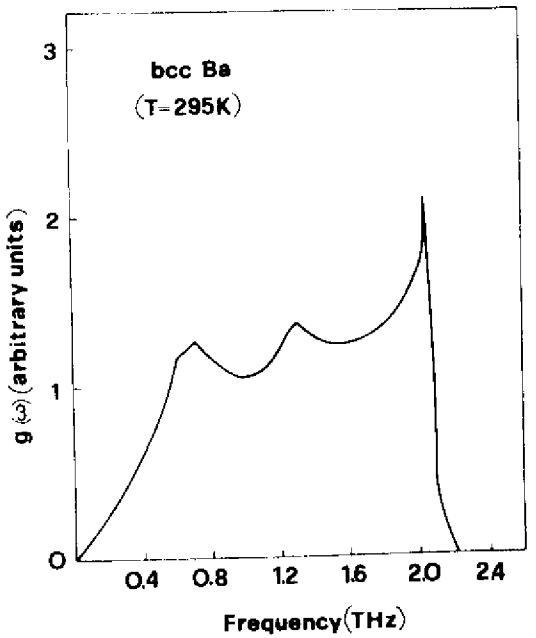
bcc Ba
(T=295K)
g (ω) (arbitrary units)
3
2
1
0
0.4
0.8
1.2
1.6
2.0
2.4
Frequency(THz)

Fig.4

Stampato in proprio nella tipografia
del Centro Internazionale di Fisica Teorica